

# Mapping Atmospheric Gravity Wave Activity with Limb-Viewing Microwave Radiometer (UARS MLS)

Dong L. Wu and Jonathan H. Jiang

Mail Stop 183-701, Jet Propulsion Laboratory, California Institute of Technology, Pasadena, CA 91109

Tel: (818)-393-1954, Email: [dwu@mls.jpl.nasa.gov](mailto:dwu@mls.jpl.nasa.gov)

## 1. INTRODUCTION

The Upper Atmosphere Research Satellite Microwave Limb Sounder (UARS MLS), operated since September 1991, has three double-sideband radiometers measuring atmospheric O<sub>2</sub>, O<sub>3</sub>, ClO, and H<sub>2</sub>O features near 63, 183 and 205 GHz [1,2]. The 63-GHz radiometer has 15 spectral channels with channel 8 centered at the center of O<sub>2</sub> lines and channels 1/15 at  $\pm 200$  MHz from the center. In the normal operation MLS step-scans atmospheric limb from 90 km to the surface in 65 seconds with  $\sim 2$  second integration time on each measurement. The limb radiances become saturated as the antenna views tangent heights near the surface. Showing little dependence on pointing, the saturated radiance basically measures atmospheric temperature of the saturation layer. Radiance fluctuations, therefore, can be reported as temperature fluctuations at that layer plus instrument noise. Depending on transmittance, radiances of different spectral channels are saturated at different altitudes and the MLS 15 channels give 8 atmospheric layers with thickness of  $\sim 10$  km (at  $\sim 28, 33, 38, 43, 48, 53, 61$  km) and  $\sim 15$  km (at 80 km). In addition to limb-scan operation, MLS has also been operated with the so-called limb-track mode in which the antenna tracks a constant tangent height (often at  $\sim 18$  km) for at least one day. The limb-track mode was mostly used during the later years of the UARS mission when its power consumption was limited. The broadside of MLS antenna, pointing at  $90^\circ$  from the satellite velocity, always views the orbital side opposite to the Sun, producing latitudinal coverage from  $34^\circ$  in one hemisphere to  $80^\circ$  in the other.

Recently, Wu and Waters [3,4] analyzed MLS radiance fluctuations and interpreted them as temperature perturbations induced by atmospheric gravity waves. The scales of these waves are often too small to measure by satellite sensors and the early observations of gravity waves are mostly from ground-based techniques. Gravity waves are of great interest to atmospheric scientists in studying atmospheric circulation and constituent mixing [5]. Understanding radiance fluctuations also has important implication to atmospheric temperature measurement. As instrument noise is continuously improved, atmospheric

fluctuations have become the dominating error source in temperature retrievals. For example, one might find that the error budget is often latitude-and-season dependent in a  $\chi^2$  analysis, which could readily be caused by gravity wave activity.

This paper describes various variance analysis techniques that have been applied to MLS radiances and provides some interpretation of observed features in terms of temperature weighting function, sampling pattern and wave propagation. MLS two-dimensional weighting functions, obtained from high-resolution radiative transfer calculations, need to be convolved with artificially-generated waves to calculate MLS filter functions to small-scale waves. Because the weighting function is tilted with respect to a local observer [Figure 1], the filter functions will depend on wave propagation direction, horizontal and vertical wavelengths, and sampling schemes used (i.e., limb-scan or limb-track).

## 2. VARIANCE ANALYSES OF MLS RADIANCES

The radiance measurements, usually taken at different locations, produce variances ( $\sigma^2$ ) that have two components mostly due to atmospheric fluctuations and instrument noise, namely,

$$\sigma^2 = \sigma_A^2 + \sigma_N^2 \quad (1)$$

The noise contribution ( $\sigma_N^2$ ) is stable, well calibrated during the flight, and independent of time and location. It can be considered as the minimum value of the radiance variances. On the other hand, the atmospheric component,  $\sigma_A^2$ , may vary with latitude, longitude and time, and depend upon the method used for calculating it. In fact, we have used several methods for the variance computation, and they are summarized in the following.

### 2.1 Single-Channel $\chi^2$ Analysis

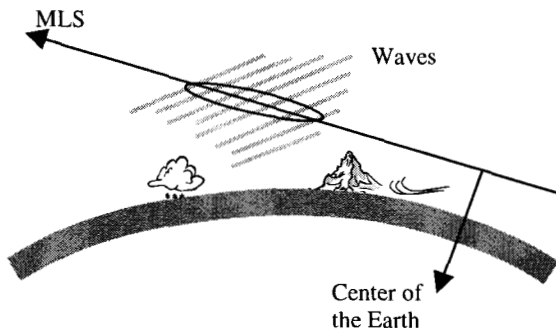
Wu and Waters [3] applied a 6-point technique to the limb-scan radiances at tangent heights below 18 km for every single scan. Their approach can be written in the following expression:

$$\begin{aligned} \tilde{\sigma}^2 &= \frac{1}{n-2} \sum_{i=1}^n (y_i - a - bz_i)^2 \\ &= \tilde{\sigma}_A^2 + \tilde{\sigma}_N^2 \end{aligned} \quad (2)$$

where the estimated variance ( $\tilde{\sigma}^2$ ) is essentially the reduced  $\chi^2$  after fitted to a linear model. Here,  $y_i$  and  $z_i$  are, respectively, radiance and tangent height. The number of radiances used is denoted by  $n$  and other parameters ( $a$  and  $b$ ) are determined from the least squares fit to the radiances. This approach uses a linear data model to remove weak tangent pressure dependence and large-scale variations to preserve small-scale wave components.

Radiative transfer calculations show that the linear model is a good approximation for the weak pressure dependence in the

Figure 1



saturated radiances as long as optical depth is greater than  $\sim 5$ . Depending on the number of the saturated radiances used, this method yields a sharp truncation to large-scale perturbations while preserving information on small scales. However, the max number of the saturated radiances that are available in the limb-scan mode is limited. It varies from 4 in channels 1/15 to  $\sim 20$  in channel 8. Such limitation puts a constraint on MLS variances such that the variance signal-to-noise (S/N) ratio for detecting small-scale fluctuations is not very high. Because atmospheric fluctuations are often weak, one would like to increase the ratio whenever possible.

## 2.2 Two-Channel $\chi^2$ Analysis

One way to increase the variance S/N ratio is to combine radiances from paired channels (e.g., channels 1 and 15). Since MLS spectral channels are symmetric about the  $O_2$  line center (channel 8), the paired channels have similar absorption coefficients and saturation altitudes. Combining these radiances will double the coherent component (atmospheric waves), analytically,

$$\begin{aligned}\tilde{\sigma}_c^2 &= \frac{1}{2(n-2)} \sum_{i=1}^n (y_{1i} - a_1 - b_1 z_{1i} + y_{2i} - a_2 - b_2 z_{2i})^2 \\ &= 2\tilde{\sigma}_A^2 + \tilde{\sigma}_N^2\end{aligned}\quad (3)$$

where the atmospheric component ( $\tilde{\sigma}_c^2$ ) in this case is twice as much as one from the single channel analysis.

## 2.3 Two-Scan $\chi^2$ Analysis

Another way to increase the S/N ratio is to use the saturated radiances from adjacent scans. The two adjacent scans are usually separated by  $\sim 500$ km due to the spacecraft movement (7.5 km/s). Because the amplitude of atmospheric fluctuations often increase with wave scale, larger spatial separation could yield a greater atmospheric variance so as to increase the S/N ratio. This approach can be written as follows:

$$\tilde{\sigma}_s^2 = \frac{1}{n-1} \sum_{i=1}^n (y_{1i} - y_{2i} - a)^2 \quad (4)$$

where the variance ( $\tilde{\sigma}_s^2$ ) is computed after removing the average (or  $a$ ) of  $y_{1i} - y_{2i}$ .

As in the methods above, this approach also uses a linear model for the weak pressure dependence, which will be removed in the differences  $y_{1i} - y_{2i}$ . By generalizing the linear model to a distance of  $\sim 500$ km, one would expect more contributions from large-scale waves and therefore must take into account gravity wave spectral density when interpreting the data.

## 2.4 Limb-Track Variances

Unlike the limb-scan cases, saturated limb-track radiances are affected much less by pointing because of the narrower range of tangent height variation. One may not need a linear model in the variance analysis. In this case, computing the small-scale variances is relatively simple. One may use the methods like Fast Fourier Transform (FFT) or running-window means to remove unwanted large-scale wave components [6]. By selecting length of the truncation windows, one can produce radiance variances

associated with different horizontal scales. Because gravity wave sources (such as convection, topography and jetstream) likely have different scales, such variance analysis can provide additional information on gravity wave properties.

Figure 2 is an example of MLS limb-track radiances taken on 4 March 1995. Tangent altitudes and radiances are shown in the top and middle panels. The bottom panel is the radiance perturbation with large ( $>1000$ km) scale waves removed. The channel numbers are labeled on the left side of the time series. Radiance perturbations of different channels are offset by a 5K increment from channel 3, showing wave amplitude growth and phase tilted with respect to height/channel.

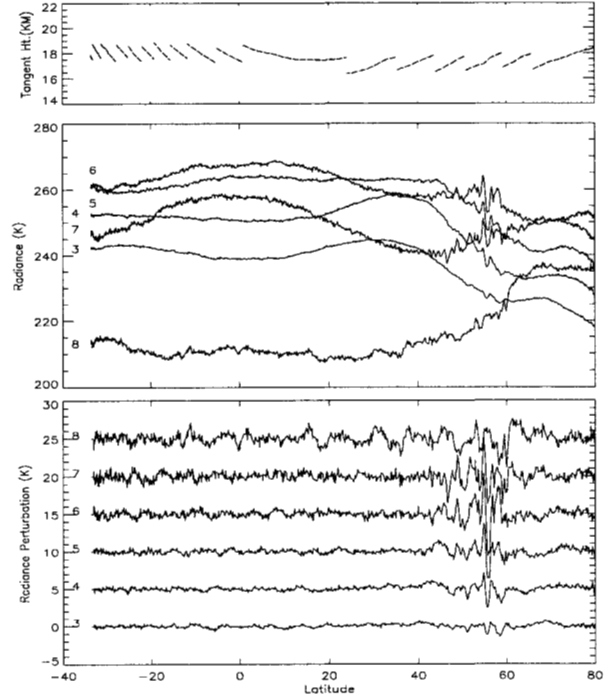


Figure 2

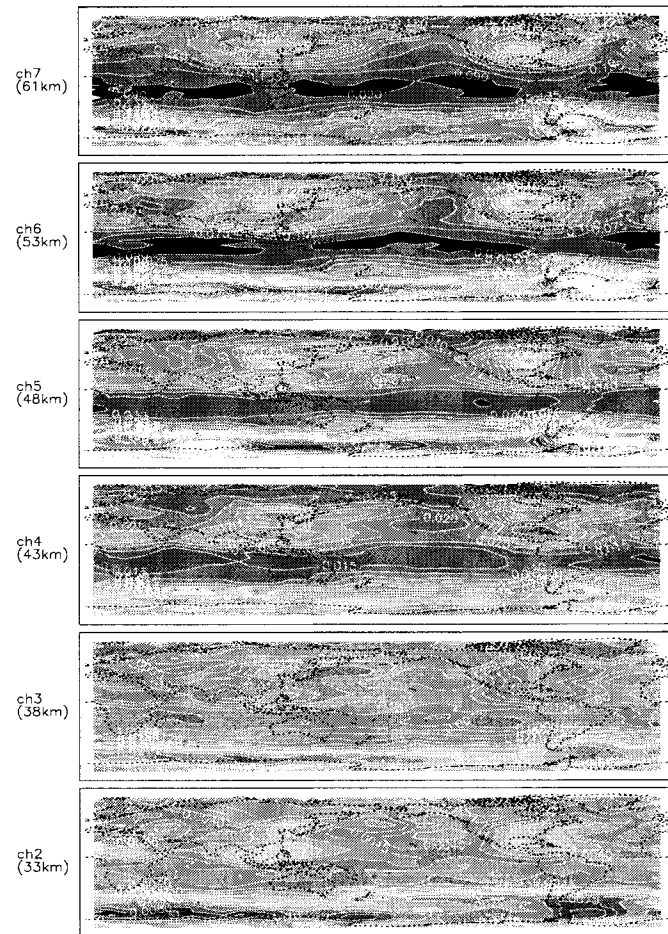
## 3. MLS FILTER FUNCTIONS

Figure 3 displays a calculated MLS filter function for the limb-scan variances using the method in section 2.1. The viewing angle is defined as the angle between light-of-sight direction and horizontal wave phase velocity. The filter function cuts off waves at small vertical/horizontal wavelengths due to the finite field-of-view ( $\sim 10$ km/ $30$ km) of MLS antenna pattern. At large horizontal wavelengths the cutoff is resulted from the truncation on the number of radiances used. Generally speaking, the variance in section 2.1 represents the waves of long ( $>10$ km) vertical and short ( $\sim 100$ km) horizontal scales. Because of the volume average by MLS weighting function ( $200$ km long,  $30$ km wide, and  $10$ km thick), the radiance responses to wave perturbations are very weak in amplitude, which needs low instrument noise and good statistics to detect.

Figure 4 is the radiance variance response as a function of viewing angle after integrating over all horizontal wavelengths (assuming a  $k_h^{-2}$  power density spectrum). The limb-scan and

**Figure 3:** A contour plot titled "Viewing Angle = 110.". The y-axis is labeled "VERTICAL WAVELENGTH (KM)" and ranges from 0 to 60. The x-axis is labeled "HORIZONTAL WAVELENGTH (KM)" and ranges from 0 to 600. Contour lines represent constant values of  $\frac{W_v}{W_h}$ , with labels including 0.0001, 0.001, 0.01, 0.05, 0.1, 0.2, 0.3, 0.4, 0.5, 0.6, 0.7, 0.8, 0.9, and 1.0.

**Figure 4:** A line graph titled "Vertical Wavelength = 15 KM". The y-axis is labeled "VARIANCE RESPONSE TO 1K WAVE" and ranges from 0.000 to 0.050. The x-axis is labeled "VIEWING ANGLE (DEGREES)" and ranges from 60 to 360. Two curves are shown: a dashed line for "SCAN MODE" which peaks at approximately 0.025 around 120 degrees, and a solid line for "TRACK MODE" which has a much smaller peak of about 0.005 around 150 degrees.



MLS filter function is key to interpreting the variances calculated. In addition to limb-scan and limb-track variance differences, we also found large differences in the variances observed between ascending and descending orbits, between upward and downward scan operations, and between MLS south-looking and north-looking periods. Most of these differences can be explained by the asymmetric filter functions

## 4. RESULTS AND INTERPRETATIONS

$$|\tilde{\sigma}^2 - \sigma^2| \approx \sqrt{2}\sigma^2 \quad (5)$$

Figure 5 shows a seasonal (JJA'92-94) map of ascending-orbit limb-scan radiance variances (using the method in section 2.3). As seen at 33-38km, the variance patterns are correlated very well with deep convection patterns in the Northern Hemisphere. In the Southern Hemisphere, the enhancement is strongly associated with stratospheric jet stream at high latitudes. In the stratosphere, the gravity wave variances seen by MLS are strongly modulated by the background winds, which is thought mainly due to a Doppler-shift effect on the wave vertical wavenumber spectrum [7].

- [1] Waters, J. W., *Atmospheric Remote Sensing by Microwave Radiometry*, M.A. Janssen, Ed. (Wiley, New York, 1993), chap.8.
- [2] Barath, F.T., et al., The Upper Atmosphere Research Satellite Microwave Limb Sounder instrument, *J. Geophys. Res.* 98, 10,751-10,762, 1993.
- [3] Wu, D. L., and J.W. Waters, Satellite observations of atmospheric variances: A possible indication of gravity waves, *Geophys. Res. Lett.*, **23**, 3631-3634, 1996a.
- [4] Wu, D. L., and J.W. Waters, Gravity-wave-scale temperature fluctuations seen by the UARS MLS, *Geophys. Res. Lett.*, **23**, 3289-3292, 1996b.
- [5] Lindzen, R.S., Turbulence and stress owing to gravity wave and tidal breakdown, *J. Geophys. Res.*, 86, 9707-9714, 1981.
- [6] McLandress, C., MJ Alexander, DL Wu, MLS observations of gravity waves in the stratosphere: A climatology and interpretation. *JGR*, in press, 2000.
- [7] Alexander, M. J., Interpretations of observed climatological patterns in stratospheric gravity wave variance. *J. Geophys. Res.*, 103, 8627-8640, 1998.